

finite and continuous at zero energy. Other theories based on atomic motion have been proposed: P. Fulde and H. Wagner, *Phys. Rev. Lett.* 27, 1280 (1971); P. W.

Anderson, B. I. Halperin, and C. M. Varma, to be published.

¹²N. F. Mott, *Phil. Mag.* 19, 835 (1969).

Spin-Wave Theory and Static Correlations in a One-Dimensional Heisenberg Antiferromagnet*

Peter M. Richards†

Sandia Laboratories, Albuquerque, New Mexico 87115

(Received 15 November 1971)

The spin-wave spectrum of a one-dimensional Heisenberg antiferromagnet with no long-range order is derived by decoupling Green's-function equations in second order. Results are applied to static correlations, and agreement is obtained with Fisher's classical solution and quasielastic neutron-scattering data in $(\text{CD}_3)_4\text{NMnCl}_3$.

We derive here a temperature-dependent spin-wave spectrum for the *isotropic* one-dimensional Heisenberg antiferromagnet with no long-range order. The results are then applied to the static correlation function $\langle \vec{S}_q \cdot \vec{S}_{-q} \rangle$ as measured in quasielastic neutron scattering¹ (\vec{S}_q is the spatial Fourier transform of the spin \vec{S}_i at the lattice site \vec{r}_i), and it is shown that the exact classical solution² is reproduced at low temperature. Our spin-wave spectrum is identical in form to that for the ordered antiferromagnet³ at zero temperature and thus is in agreement with recent observations⁴ in $(\text{CD}_3)_4\text{NMnCl}_3$ (TMMC). Hence, this Letter reconciles the existence of well-defined spin waves with static correlations given by the classic model, both of which have been verified by neutron experiments on TMMC.

The experiments on TMMC have received much attention since they have shown that the idealized one-dimensional antiferromagnet is realized in practice, and a sensitive test of one-dimensional theories is thus possible. Briefly, results are in accord with Fisher's theory of static correlations for $S \rightarrow \infty$ and also demonstrate the existence of well-defined spin waves. These spin waves have the same dispersion relation as for an artificial one-dimensional antiferromagnet with long-range order, even though such order is absent in TMMC. Computer solutions to approximate integrodifferential equations for classical spins⁵ and to finite spin- $\frac{1}{2}$ chains⁶ have produced spin waves at finite temperatures, and the zero-temperature spectrum⁷ is known for spin $\frac{1}{2}$; but we know of no work prior to this which gives simple analytic expressions valid for finite temperature and arbitrary spin.

The discovery of spin waves in TMMC has posed an apparent dilemma. How can the static correlation functions of the classical theory be

compatible with spin-wave dynamics? At first glance they are quite incompatible, as we discuss below. The major thrust of this paper, apart from giving a simple derivation of the spin-wave spectrum, is to show that the static correlations do fit nicely into the framework of spin-wave theory and that our solution is identical to Fisher's for the observable parameters of quasielastic scattering in the low-temperature limit.

The apparent incompatibility of the spin-wave and classical descriptions stems from the form of $\langle \vec{S}_q \cdot \vec{S}_{-q} \rangle$ implied by the two theories and has been noted previously.⁴ The classical solution gives

$$\langle \vec{S}_q \cdot \vec{S}_{-q} \rangle = S(S+1) \left(\frac{1-u^2}{1+u^2+2u \cos qa} \right) \quad (1)$$

with $u = \coth K - 1/K$ and $K = 2JS(S+1)/k_B T$, where, in our notation, the exchange interaction J is positive for antiferromagnetic coupling so that u is positive for the case of interest. The quantity a is the nearest-neighbor spacing and J is assumed to be confined to the two nearest neighbors on a linear chain. Equation (1) predicts maximum correlation at $q = \pi/a$, the same as for an ordered antiferromagnet and as confirmed by quasielastic neutron scattering.¹ For small $\tilde{q} = \pi/a - q$, a Lorentzian

$$\langle \vec{S}_q \cdot \vec{S}_{-q} \rangle \propto (\tilde{q}^2 + \kappa^2)^{-1} \quad (2)$$

results with the inverse correlation length κ given by

$$\kappa = (1-u)/\sqrt{u}a. \quad (3)$$

The staggered ($q = \pi/a$) susceptibility is thus finite at nonzero temperature.

Spin-wave theory for a one-dimensional anti-

ferromagnet with long-range order predicts^{3,4}

$$\langle S_{q_+} S_{q_-} \rangle = 4JS^2(1 - \cos qa)(2n_q + 1)/\hbar\omega_q \quad (4)$$

for the transverse correlations, where $n_q = [\exp(\hbar \times \omega_q/k_B T) - 1]^{-1}$. The spin-wave frequency is $\omega_q = 4(J/\hbar)S \sin qa$. It is evident from (4) that a maximum occurs at $q = \pi/a \equiv q_0$, but $\langle S_{q_0+} S_{q_0-} \rangle$ —and thus the staggered susceptibility—diverges at all temperatures so that the correlation length κ^{-1} is infinite at all temperatures.

The key to the difference between Eqs. (1) and (4) is the fact that simple wave theory gives $\omega_q = 0$ at $q = \pi/a$. An energy renormalization which is wave-vector independent will not change this result. The spin-wave spectrum derived below, however, shows a renormalization which depends on q . In particular, we find $\omega_{q_0} \propto T$. This gives rise to a finite staggered susceptibility and leads to the form (2) with the same value for κ as in (3) in the low-temperature limit. The correlation $\langle \vec{S}_{q_0} \cdot \vec{S}_{-q_0} \rangle$ is also shown to have the same temperature dependence as predicted by the classical model (1).

Calculation of the spin-wave frequency proceeds by decoupling Green's-function equations of motion in second order. The Green's function $G_q^{(n)}(t)$ is defined in the usual way⁸ as

$$G_q^{(n)}(t) = -i \langle [d^n S_{q_+}(t)/dt^n, S_{q_-}(0)] \theta(t) \rangle, \quad (5)$$

where $\theta(t)$ is the unit step function.

Since there is no long-range order, it is not fruitful to decouple in lowest order [$G_q^{(1)}(\omega) \sim \langle S_z \rangle G_q^{(0)}(\omega)$]. Second-order decoupling⁹ is possible according to the scheme

$$S_{q_1+} S_{q_2-} S_{q_3+} + \langle S_{q_1+} S_{q_1-} \rangle S_{q_3+} \delta_{q_1, q_2} \\ + \langle S_{q_2-} S_{q_2+} \rangle S_{q_1+} \delta_{q_2, q_3}$$

and

$$S_{q_1z} S_{-q_2z} S_{q_3+} + \langle S_{q_1z} S_{-q_1z} \rangle S_{q_3+} \delta_{q_1, q_2}.$$

This procedure yields

$$G_q^{(2)}(\omega) = -\omega_q^{-2} G_q^{(0)}(\omega), \quad (6)$$

for the frequency-dependent function in which

$$\hbar^2 \omega_q^{-2} = \frac{16}{3} S(S+1) J^2 (1 + \tau_2) \\ \times [1 - \cos^2 qa + \lambda(\cos^2 qa - \cos qa)], \quad (7)$$

where $\lambda = (1 + 2\tau_1 + \tau_2)/(1 + \tau_2)$, and isotropy has been assumed. The quantities τ_1 and τ_2 are normalized first- and second-neighbor correlations: $\tau_j = \langle \vec{S}_i \cdot \vec{S}_{i+j} \rangle / S(S+1)$. The exact classical solution has $\tau_1 = -u$, $\tau_2 = u^2$. At zero temperature λ

= 0 for the classical system so that

$$\omega_q(0) = (4J/\hbar) [\frac{2}{3} S(S+1)]^{1/2} \sin qa. \quad (8)$$

In the limit $S \rightarrow \infty$, $\omega_q(0)$ is less than the Anderson value $(4J/\hbar)S \sin qa$ by the factor $\sqrt{\frac{2}{3}}$; but for $S = \frac{5}{2}$, the factor is $\sqrt{\frac{14}{15}} = 0.965$, so the result (8) is very close to the ordered spectrum for TMMC.

Equation (7) shows ω_q to be temperature dependent. This produces a relatively small renormalization of long-wavelength ($q < \pi/2a$) spin waves and, more important, makes $\omega_q \neq 0$ at $q_0 = \pi/a$. The renormalization is 8.5% for $q = \pi/8a$ at $T = 20$ K in TMMC, perhaps in reasonable accord with the failure⁴ to observe any temperature dependence of ω_q up to 20 K. At q_0 the frequency is

$$\omega_{q_0} = 4[\frac{2}{3} S(S+1)]^{1/2} (J/\hbar) (1 - u) \\ \approx 2\sqrt{\frac{2}{3}} k_B T / [S(S+1)]^{1/2} \hbar, \quad (9)$$

where the classical values for τ_1 and τ_2 have been used. The linear temperature dependence expressed in (9) is an excellent approximation for all temperatures of interest since corrections are of the order of $e^{-2K} = e^{-6.75}$ at $T = 40$ K in TMMC. As a result, n_{q_0} is independent of T . The decoupling (6) enables one to solve for $G_q^{(0)}(\omega)$. The static correlation $\langle S_{q_+} S_{q_-} \rangle$ is then determined by standard spectral-density theorems.⁸ We find

$$\langle \vec{S}_q \cdot \vec{S}_{-q} \rangle = 4J |\tau_1| S(S+1) \\ \times (1 - \cos qa)(2n_q + 1)/\hbar\omega_q \quad (10)$$

after using isotropy [$\langle \vec{S}_q \cdot \vec{S}_{-q} \rangle = \frac{3}{2} \langle S_{q_+} S_{q_-} \rangle$]. Use of (9) in (10) then gives

$$\langle \vec{S}_{q_0} \cdot \vec{S}_{-q_0} \rangle = 4Ju\sqrt{\frac{3}{2}} [S(S+1)]^{3/2} \\ \times \coth[\frac{2}{3} S(S+1)]^{1/2} / k_B T \quad (11)$$

for the classical value $\tau_1 = -u$. In the limit of large S and $T \rightarrow 0$, the above reduces to $\langle \vec{S}_{q_0} \cdot \vec{S}_{-q_0} \rangle = 6JS^2(S+1)^2/k_B T$ which differs from (1) only in the coefficient of J , which is 4 for the exact classical solution. The discrepancy of a factor of $\frac{3}{2}$ does not, of course, affect the experimentally observable temperature dependence of $\langle \vec{S}_{q_0} \cdot \vec{S}_{-q_0} \rangle$. Figure 1 gives a comparison between Eqs. (11) and (1) for the temperature dependence of $\langle \vec{S}_{q_0} \cdot \vec{S}_{-q_0} \rangle$, proportional to the inverse of the peak quasielastic scattering intensity. The curves are normalized to give the same slope at $T \rightarrow 0$. Data from Ref. 1 are also shown.

The correlation length κ^{-1} is determined by expanding Eq. (10) to lowest order in $\tilde{q} = \pi/a - q$ and comparing the result with the form (2). In this

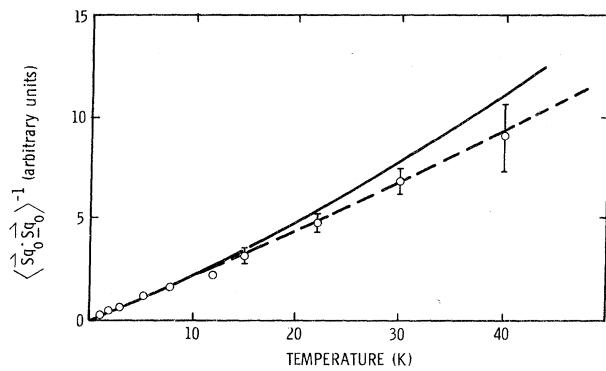


FIG. 1. Inverse static correlation $\langle \vec{S}_{q_0} \cdot \vec{S}_{-q_0} \rangle^{-1}$ at $q_0 = \pi/a$. Solid curve is spin-wave theory, Eq. (11). Dashed curve is exact classical result, Eq. (1). Curves have been normalized to give the same slope at $T=0$. Experimental points are from Ref. 1.

way we obtain

$$(\kappa a)^{-2} = \frac{1}{4} \left(\frac{1+u}{1-u} \right)^2 \left[\frac{1 + \hbar\omega_{q_0}}{k_B T \sinh(\hbar\omega_{q_0}/k_B T)} \right] - \frac{1}{8} \left[\frac{1 + 3\hbar\omega_{q_0}}{k_B T \sinh(\hbar\omega_{q_0}/k_B T)} \right]. \quad (12)$$

For large S and $T \rightarrow 0$, Eq. (12) gives identically the same value for κ as the classical model (3). There is only a 2% difference between (12) and (3) for $S = \frac{5}{2}$ and $T \rightarrow 0$. Figure 2 shows the inverse correlation length κ vs T for TMMC as given by both by spin-wave theory (12) and the exact classical result (3). Data from Ref. 1 also are presented.

Data in both figures favor the classical model, but the spin-wave curve nearly lies within the error bars. A more rigorous theory for the temperature dependence of ω_{q_0} might be expected to give better agreement with the classical model at the high temperatures.

In Figs. 1 and 2 the value $J/k_B = 7.7$ K has been used in accordance with quasielastic results of Ref. 1. Hutchings *et al.*⁴ deduced $J/k_B = 6.6$ K from the measured dispersion relation $\hbar\omega_q/k_B = 4S(7.07) \sin qa$ and the theoretical expression $\hbar\omega_q = 4JS(1.07) \sin qa$ based on spin-wave theory for an ordered antiferromagnet including correction terms. Our relation (8) together with the observed spectrum gives $J/k_B = 7.3$ K so that better consistency is obtained between the two neutron experiments. The neutron-data values remain significantly above the figure² of $J/k_B = 6.47$ K inferred from static susceptibility measurements.¹⁰ This discrepancy might have to do with the temperature dependence of J since the susceptibility

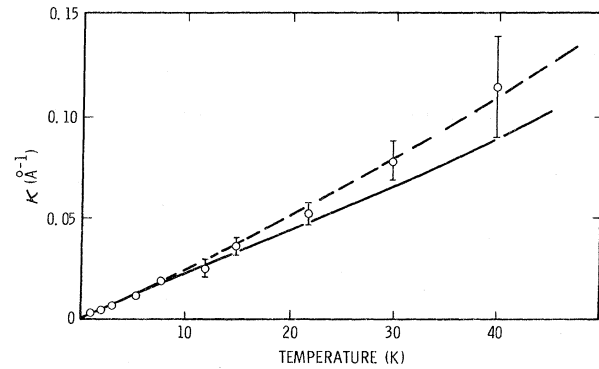


FIG. 2. Inverse correlation length κ . Solid curve is spin-wave theory, Eq. (12). Dashed curve is exact classical result, Eq. (3). Experimental points are from Ref. 1.

data were analyzed between 170 and 60 K.

In conclusion, we have demonstrated that a simple second-order Green's-function decoupling scheme gives rise to a spin-wave spectrum which agrees with the inelastic neutron scattering data. It has not been necessary to assume the existence of long-range order. Perhaps more significant is the fact that this spectrum also is able to explain quite well the quasielastic data on temperature dependence of $\langle \vec{S}_{q_0} \cdot \vec{S}_{-q_0} \rangle$ and the absolute value and temperature dependence of correlation length κ^{-1} . It had previously been thought that spin-wave theory could not account for these features; and indeed it cannot unless a wave-vector-dependent renormalization is used, such as naturally occurs in our formalism. This renormalization has the physically attractive feature of making the staggered susceptibility finite at finite temperature. The simple approximation employed here does not allow for damping effects. A more detailed calculation, such as undertaken by McClean and Blume,⁵ is necessary to account for broadening of the spin-wave peak at higher temperatures.

*Work supported by the U. S. Atomic Energy Commission.

†Permanent address: Department of Physics, University of Kansas, Lawrence, Kans. 66044.

¹R. J. Birgeneau, R. Dingle, M. T. Hutchings, G. Shirane, and S. L. Holt, *Phys. Rev. Lett.* **26**, 718 (1971).

²M. E. Fisher, *Amer. J. Phys.* **32**, 343 (1964).

³P. W. Anderson, *Phys. Rev.* **86**, 694 (1952).

⁴M. T. Hutchings, G. Shirane, R. J. Birgeneau, and S. L. Holt, *Phys. Rev. B* (to be published), and a preliminary account given in *J. Appl. Phys.* **42**, 1265 (1971).

⁵F. B. McClean and M. Blume, *J. Appl. Phys.* **42**, 1380 (1971).

⁶P. M. Richards and F. Carboni, *Phys. Rev. B* (to be published).

⁷J. des Cloizeaux and J. J. Pearson, *Phys. Rev.* **128**, 2131 (1962).

⁸D. N. Zubarev, *Usp. Fiz. Nauk* **71**, 71 (1960) [*Sov. Phys. Usp.* **3**, 320 (1960)]; see also L. P. Kadanoff and G. Baym, *Quantum Statistical Mechanics* (Benjamin, New York, 1962).

⁹This decoupling procedure has recently been used by S. K. Lo and J. W. Halley, in Proceedings of the Seventeenth Conference on Magnetism and Magnetic Materials, Chicago, November 1971 (American Institute of Physics, New York, to be published), in a treatment of the three-dimensional Heisenberg paramagnet.

¹⁰R. Dingle, M. E. Lines, and S. L. Holt, *Phys. Rev.* **187**, 643 (1969).

Acoustic-Phonon Instability and Critical Scattering in $\text{Nb}_3\text{Sb}^\dagger$

G. Shirane and J. D. Axe

Brookhaven National Laboratory, Upton, New York 11973

(Received 21 October 1971)

Neutron-scattering experiments on Nb_3Sn show the drastic softening of the [110] acoustic shear modes as well as an unusual frequency response (a central peak in addition to the phonon side bands) near the phase transition at 45°K. A model involving coupling of the bare phonon to other fluctuations with a Debye-like frequency spectrum is proposed which correctly describes the observed cross section as a function of temperature.

The structural phase transition in the high-temperature superconductor Nb_3Sn is characterized by a drastic softening¹ of the acoustic shear mode with vector $\vec{q} \parallel [110]$ and polarization vector $\vec{e} \parallel [1\bar{1}0]$. At the transition temperature $T_m = 45^\circ\text{K}$, the crystal structure changes from a cubic to a slightly distorted tetragonal structure.² In a recent neutron-diffraction study,³ we have determined the atomic displacements in the tetragonal phase and concluded that only an acoustic instability (not an optic one) is required to explain the transition.⁴ This paper reports some unusual dynamical characteristics of these soft shear modes revealed by inelastic neutron-scattering techniques.

Experiments were carried out on a triple-axis spectrometer at the Brookhaven high-flux beam reactor on the same single crystal used in our recent study.³ The crystal was grown by Hanak and Berman⁵ and has a volume of 0.05 cm³, small for inelastic neutron-scattering experiments. Bent-focusing pyrolytic graphite monochromator crystals were used with incoming neutron energies of 40, 14, and 5 meV.

The temperature dependence of the [110] transverse acoustic (TA) branch is shown in Fig. 1. First we note a relatively large decrease of phonon energies on cooling for high ζ values. Here the wave vector \vec{q} is expressed as $(\zeta, \zeta, 0)2\pi/a$. This decrease, about 15%, persists up to the zone boundary, $\zeta = 0.5$. A similar decrease was also observed for phonons in the [100] transverse acoustic branch; for example, the phonon energies at the zone boundaries are 7.5 and 6.5 meV at 295 and

46°K, respectively. Thus, there seems to be a substantial softening over the entire range of wave vectors. This is unexpected and not at all understood at present.

Much more drastic softening was observed for the [110] branch for smaller ζ values. The general characteristics of the temperature depen-

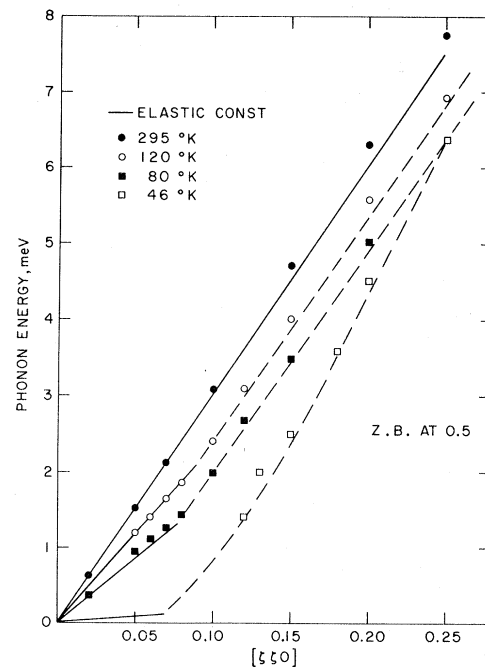


FIG. 1. Temperature dependence of TA modes along $\vec{q} = (\zeta, \zeta, 0)2\pi/a$ with polarization vector $\vec{e} \parallel [1\bar{1}0]$. $2\pi/a = 1.19 \text{ \AA}^{-1}$ at 46°K.